Applied Catalysis B: Environmental 134–135 (2013) 123–129

Contents lists available at SciVerse ScienceDirect

Applied Catalysis B: Environmental

journal homepage: www.elsevier.com/locate/apcatb

Preparation of alumina-supported gold-ruthenium bimetallic catalysts by redox reactions and their activity in preferential CO oxidation

O.A. Kirichenko[a], E.A. Redina[a], N.A. Davshan[a], I.V. Mishin[a], G.I. Kapustin[a], T.R. Brueva[a], L.M. Kustov[a,b,*], Wei Li[c], Chang Hwan Kim[c]

[a] N.D. Zelinsky Institute of Organic Chemistry, Russian Academy of Sciences, 47 Leninsky prospect, Moscow, 119991, Russian Federation
[b] Chemistry Department, Moscow State University, 1 Leninskie Gory, bldg. 3, Moscow, 119992, Russian Federation
[c] General Motors Global Research and Development, Chemical Sciences & Materials Systems Laboratory, 30500 Mound Rd., Warren, MI 48090, USA

ARTICLE INFO

Article history:
Received 5 September 2012
Received in revised form
25 December 2012
Accepted 29 December 2012
Available online 4 January 2013

Keywords:
Bimetallic catalysts
Gold-ruthenium/alumina
CO oxidation
Ammonia oxidation

ABSTRACT

Lean-burn engine technology offers improved fuel economy; however, the reduction of NO_x during lean-operation continues to be a major technical hurdle in the implementation of energy efficient technology. Recently reported passive NH_3-SCR system (PASS)– a simple, low-cost, and urea-free system – has the potential to enable the implementation of lean-burn gasoline engines; however, the system suffers from CO slips during extended rich operations. The slipped CO can be easily oxidized with supplemental oxygen feed over platinum group metal (PGM)-based catalysts; however the PGM-based catalysts simultaneously oxidize the generated NH_3. This work focuses on the preparation of catalysts that can preferentially oxidize CO in the presence of NH_3.

Highly active bimetallic Au-Ru/Al_2O_3 catalysts were prepared by the method of $[AuCl_4]^-$ reduction by hydrogen preadsorbed on a parent monometallic Ru/Al_2O_3 catalyst serving as a carrier. The temperature-programmed reduction studies confirmed a strong interaction between the Au and Ru particles in the samples prepared by this redox method. The average size of crystallites was less than 7 nm and 20 nm for Au and Ru, respectively. The activity of the catalysts was studied in the reaction of oxidation of a mixture of CO with NH_3. The catalytic activity in CO oxidation was found to be higher over the bimetallic Au-Ru/Al_2O_3 catalyst compared to the monometallic Ru/Al_2O_3 and Au/Al_2O_3 catalysts. On the contrary, in NH_3 oxidation, the bimetallic Au-Ru/Al_2O_3 catalyst exhibited a decreased activity compared to the relevant monometallic catalysts. Preparation of Au-Ru/Al_2O_3 samples by the commonly used method of deposition-precipitation with urea resulted in the less catalytically active samples due to the formation of larger Au particles and their separate deposition from Ru.

1. Introduction

The fuel economy of spark-ignition engine applications can be further improved through the use of extended lean operation. The fuel economy potential of stratified-charge engine concepts has been widely documented. Lean burn spark-ignition direct injection (SIDI) engines offer significant fuel efficiency benefits that can contribute to a reduction in greenhouse gas emissions by carrying out fuel combustion in excess air. Unfortunately, a major by-product of lean combustion is NO_x ($x = 1, 2$), the aftertreatment of which remains a major challenge. By some accounts, the lack of cost-effective NO_x aftertreatment materials and technologies is the key obstacle to broader implementation of fuel efficient lean-burn SIDI engines.

Recently, the General Motors stratified lean SIDI aftertreatment team demonstrated the concept of passive NH_3 SCR system (PASS) coupled with a conventional three-way catalyst (TWC) [1]. The PASS system operates by the following key strategic steps:

1. Periodically the engine operates slightly rich of stoichiometric air-to-fuel ratio to produce NH_3 on the TWC using engine out NO_x and H_2;
2. The produced NH_3 is stored on the downstream SCR catalyst;
3. During subsequent lean operations the NO_x emissions are converted to N_2 over the SCR catalyst by using the stored reductant, NH_3.

However, the innovative system suffers from the large amount of CO slip under extended rich operations that are required for the NH_3 production. In conventional TWC system, oxygen storage material such as CeO_2 has been effective to remove CO under short period of rich-bias operations, however for the PASS system, the

* Corresponding author. Tel.: +7 9104140702; fax: +7 4991355328.
E-mail address: LMK@ioc.ac.ru (L.M. Kustov).

0926-3373/$ – see front matter © 2013 Elsevier B.V. All rights reserved.
http://dx.doi.org/10.1016/j.apcatb.2012.12.039

oxygen storage material cannot handle under the richer and longer period of rich operation. Further, the NH_3 yield is maximized when oxygen storage material is completely depleted. The only way of removing CO during the rich operation will be the water gas shift reaction. However, the WGS reaction is not favorable, at least not effective under the temperature range for the PASS system, because the conversion of CO is limited by its thermodynamic equilibrium. One potential solution is to place another oxidation catalyst in the underflow location, between TWC and SCR catalysts, with external oxygen supply. At the time when the slipped CO flows through the catalyst, NH_3 is also present in the exhaust. In the PASS system, the oxidation of NH_3 has to be avoided as we consume extra fuel to generate NH_3 by running engine richer. Our preliminary measurements with a PGM-based TWC catalysts show that, simultaneously with CO oxidation, NH_3 was oxidized into NO_x. Therefore for the PASS system, it is crucial to develop a novel selective CO oxidation catalyst over NH_3. The preferential CO oxidation over such catalyst should occur in the mixture with NH_3 at the temperatures at which the almost complete CO conversion could be reached with a minimal NH_3 conversion. Considering that the optimum working temperature for SCR systems used for diesel vehicles is about 350–400 °C and can be decreased to 250 °C for the next generation of SCR catalysts [2–7], the working temperature range for the catalysts of preferential CO oxidation in the NH_3 presence seems to be 250–400 °C.

Gold nanoparticles supported onto transition metal oxides are known as efficient catalysts of CO oxidation even at room temperature, with their activity and stability being strongly dependent on the size of the particles and the nature of the metal oxide [8]. Recently the high rates of CO oxidation were also revealed at room temperature for nanoparticles of mesoporous RuO_2 [9]. In the case of Ru/Al_2O_3, CO oxidation usually occurs [10] at 120–180 °C. However, to the best of our knowledge, no data can be found in the literature related to the activity of the bimetallic Au-Ru catalyst in CO oxidation, although some enhancement of the activity of the Au-Ru catalysts in comparison with the corresponding Au and Ru monometallic systems was found in the reactions of water gas shift [11] and hydrogen production from methanol [12]. Ruthenium was claimed to play crucial role in these catalytic processes both in the metallic and in the oxide state.

The major problem faced in the preparation of bimetallic supported catalysts is the impossibility to ensure an extended area of contact of the monometallic phases in those cases when the alloy formation is not expected. The conventional method of co-impregnation of the carrier with solutions containing salts, sols or other precursors of the metals, as a rule, can hardly produce highly active bimetallic catalysts. Therefore, novel methods have been proposed for the tailored synthesis of bimetallic catalysts based on the modification of the already supported first metal with the second metal [13]. The creation of an extended contact between the two metals is favored by the surface interaction of the primary supported component with a precursor of the second metal. When the metallic phases are the goal, diverse redox methods are used that are based on the reduction of the ions of the second metal either by the pre-supported first metal [14] or by a reducing agent adsorbed at the surface of the first metal, for instance, hydrogen [15]. Such methods have been successfully used for the synthesis of Au-Pt/SiO_2 catalysts with a variable Au content [16]. It has been shown that gold deposition proceeds uniformly over the entire surface of a Pt particle at low Au contents (Au/Pt < 0.15), whereas a further increase of the Au loading results in predominant gold deposition on the atoms with a low coordination numbers. This effect is explained by the transition from the reduction with adsorbed hydrogen to the reduction by the first metal.

The objective of this work is the elaboration of a redox method for the preparation of Au–Ru bimetallic catalysts and evaluation of their activity in the preferential CO oxidation in the presence of NH_3. A comparison with the systems prepared by a conventional precipitation method using urea is also carried out.

2. Experimental

2.1. Catalyst preparation

Commercial carriers were used in the preparation of the monometallic and bimetallic catalysts: TiO_2 (P25 Degussa, Germany, $S = 45\ m^2\ g^{-1}$) and γ-Al_2O_3 (A-6, Ryazan Refinery, Russia; $S = 115\ m^2\ g^{-1}$, pore volume $0.53\ cm^3\ g^{-1}$). The high-temperature modification θ-Al_2O_3 with the specific surface area of $95\ m^2\ g^{-1}$ was prepared by thermal treatment of γ-Al_2O_3 at 1000 °C for 2 h. Ruthenium was supported by incipient wetness impregnation of θ-Al_2O_3 (particle size, 0.1–0.25 mm) in an excess of a $(NH_4)_3[Ru(C_2O_4)_3]$ solution ($C = 6.28 \times 10^{-2}$ M) with further evaporation of the solution at 80 °C under a vacuum, drying at 100 °C and calcination at 300 °C. The calcination temperature was chosen on the basis of the results of a TG/DTA analysis of decomposition of the dried sample. Two samples with the weight content of ruthenium of 1% and 5% were prepared (denoted as Ru1 and Ru5). The preparation of a $(NH_4)_3[Ru(C_2O_4)_3]$ solution was described elsewhere [17].

Deposition of gold onto TiO_2 and θ-Al_2O_3 (reference samples) was carried out by the method of deposition precipitation using urea (DPU) [18] according to a procedure described in [19]. Before performing the catalytic activity tests and X-ray diffraction analyses, the catalysts were calcined at 300 °C for 2 h that resulted in a complete reduction to Au^0 [19]. To determine the completeness of the gold deposition, an aliquot of a mother solution (2 ml) was collected and iodometric titration of gold was carried out with $Na_2S_2O_3$ [20]. The major amount of gold was deposited (98%). The Au loading was 1 wt% in all catalysts.

For the case of the carriers pre-modified with RuO_2, gold was supported by a redox method used to support noble metals on the surface of other metals, for example, for gold deposition onto platinum [16]. The samples were prepared by reduction of gold ions by metallic ruthenium and hydrogen adsorbed on ruthenium. For this purpose, the RuO_2/θ-Al_2O_3 samples were first reduced in a flow of H_2 ($60\ cm^3\ min^{-1}$) at 300 °C for 2 h. Then the reactor was cooled to room temperature and a required amount of a 9.51×10^{-3} M $HAuCl_4$ solution was introduced without a contact with air. The precipitate was separated using a centrifuge and washed with a 0.01 M NaOH solution and then with distilled water (100 ml per 1 g of the catalyst) to remove Cl^- ions. The obtained catalyst was dried at 60 °C. For comparison, the samples with the same metal loadings were prepared by Au deposition on the RuO_2/θ-Al_2O_3 supports in accordance with the DPU recipe used for the preparation of Au/δ-Al_2O_3 in [19].

2.2. Catalyst characterization

The specific surface area of the samples was determined by the BET method according to the procedure reported in [21]. The phase composition of the samples and the particle size of the supported metals were examined by X-ray diffraction (XRD) analysis. X-ray diffraction patterns were recorded using a DRON-2 diffractometer with Ni-filtered Cu Kα radiation (λ = 0.1542 nm) in a step scanning mode, with a step of 0.02° and a counting time of 0.3–0.6 s per step in the range $2\theta = 20–80°$. All major reflections of Au, Ru, and RuO_2 were covered by this scan range. The crystal size of nanoparticles was calculated from X-ray line broadening analysis.

Temperature programmed reduction (TPR) measurements were performed in a laboratory flow system [17]. A sample (100 mg) was

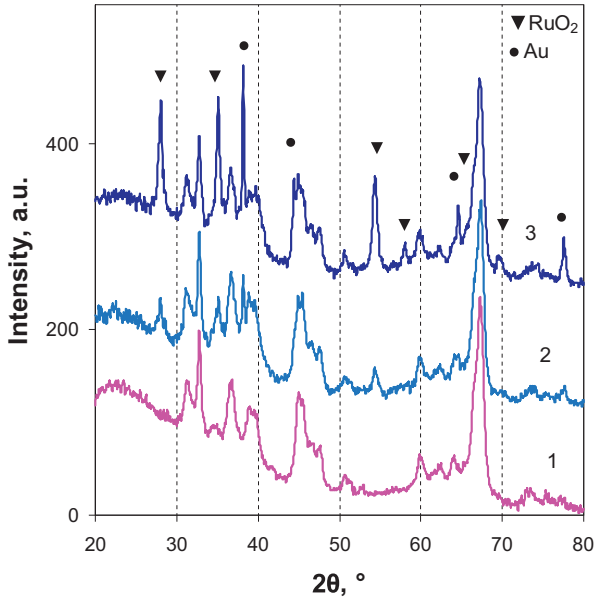

Fig. 1. XRD patterns of the samples θ-Al_2O_3 (1); AuRu1-DPU (2); AuRu5-DPU (3).

pretreated in an argon flow at 150 °C for 30 min and was cooled in Ar to −50 °C prior to the TPR experiment. Heating from −50 to 400 °C was carried out at a rate of 10 °C min^{-1} in a flow (30 cm^3 min^{-1}) of a mixture of 4.6% H_2 in Ar. Then the sample was kept at 400 °C until the completion of hydrogen consumption. An argon flow was used to avoid hydrogen absorption on precious metal atoms upon cooling [22].

2.3. Activity measurement

The prepared catalysts were tested in the reaction of oxidation of a gas mixture containing both carbon monoxide and ammonia. The variation in the conversion with temperature was studied by the point-to-point method. The catalyst testing was carried out in a microreactor system using a fixed bed quartz reactor (internal diameter 3 mm) operating at an atmospheric pressure. The feed gas mixture consisted of 1.5 vol.% NH_3, 4.5 vol.% CO, 22.5 vol.% O_2 and He balance. The total feed flow rate was maintained at 10 cm^3 min^{-1}, with a volume hourly space velocity (VHSV) of 6000 h^{-1}. The preshaped (RR) or pressed (DPU) samples were crushed and sieved into particles of a size ranging from 0.25 to 0.1 mm. The catalyst was placed on a thin layer of quartz wool in the reactor. In each test, the catalyst volume was equal to 0.1 cm^3 (the sample mass varied within 95–100 mg). Before the test, each catalyst was pretreated in a dry air flow at 300 °C for 1 h to remove water and adsorbed species, and then the reactor was cooled to room temperature. The effluent gas mixture from the reactor was analyzed using a GC (a 3700-01 chromatograph, Russia) with a TCD detector and with a molecular sieve 5A column to determine the CO conversion and a column with Hayesep to determine the NH_3 conversion.

3. Results and discussion

3.1. Phase composition of the synthesized samples

The XRD patterns of the θ-Al_2O_3 support and DPU supported gold-ruthenium catalysts are presented in Fig. 1. The reflections of metallic gold and ruthenium dioxide are observed on the background of the θ-Al_2O_3 XRD pattern for the catalysts prepared by the DPU method. This indicates the presence of large crystals. The

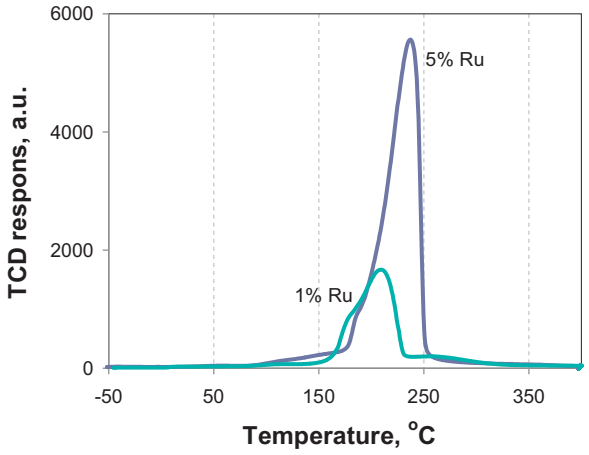

Fig. 2. TPR curves for the initial RuO_x/θ-Al_2O_3 supports (Ru1 and Ru5 samples).

calculated average size of gold particles in the sample AuRu5-DPU was over 40 nm. The formation of such big Au nanoparticles is not typical for the DPU method that has been earlier tested using oxide support of different nature and is observed for the first time. For comparison, the sample 1%Au/θ–Al_2O_3 synthesized by the DPU method in this work contained gold as the particles with a size smaller than 3 nm, as evidenced by the absence of reflections of gold on the XRD pattern of this sample (it is not presented because it coincides with the pattern for the support material). The comparison of the XRD patterns for the samples prepared by the DPU method (Fig. 1) shows that an increase in the ruthenium content causes an increase in the average size of the gold metal particles and a growth of the population of large Au particles. This can be explained by very low concentration of the centers responsible for the adsorption of the $[AuCl_4]^-$ anions on the surface of RuO_2 and blocking of the centers of adsorption of $[AuCl_4]^-$ anions by oxalate-ruthenate anions on the surface of θ-Al_2O_3 upon the preliminary introduction of Ru precursors. The decrease of the number of adsorbed $[AuCl_4]^-$ anions serving the centers of nuclei formation for the gold precursor deposited by the DPU method may have resulted finally in the growth of the depositing particles. The reason behind the poor adsorption of the $[AuCl_4]^-$ anions may be the low value of the isoelectric point of the surface (lower than the range of pH variation during the synthesis of the samples) for RuO_2 (unfortunately, we failed to find any literature data). The above reasoning makes us to assume that gold was deposited predominantly on the surface of θ-Al_2O_3 rather than on RuO_2.

Further we applied a redox method to deposit gold particles on the surface of RuO_2. Since the synthesis by this method requires the presence of pre-supported metallic ruthenium, we studied first the conditions of the reduction of RuO_2 supported onto θ-Al_2O_3. For this purpose, the method of temperature-programmed reduction was used, with the samples pre-calcined at 300 °C. The TPR curves are presented in Fig. 2, and the overall hydrogen uptake is given in Table 1. It follows from these data that virtually complete reduction of RuO_2 in a flow containing hydrogen occurs at temperatures below 300 °C. This temperature was chosen for the reduction of the samples in a hydrogen flow during the synthesis by the redox method. The values of H_2: Ru ratios for the starting samples turned out to be higher than it was expected, which indicates that extra H_2 was consumed possibly due to the presence of ruthenates and adsorbed oxygen in these samples, besides the RuO_2 phase [9].

For the successful synthesis by the redox method, reoxidation of reduced metal should be avoided, and one should also have an

Table 1
Hydrogen uptake upon reduction of the RuO_x/θ-Al_2O_3 and supported Au-Ru catalysts in the temperature range −50–400 °C.

Sample	Reduction of the starting catalyst		Reduction of the reoxidized catalyst	
	H_2 uptake (μmol g^{-1})	H_2:Ru	H_2 uptake (μmol g^{-1})	H_2:Ru
Ru5	1300	2.81	147	0.32
AuRu5-DPU	1200	2.61	137	0.30
AuRu5-RR calcined at 500 °C	955	2.06	71	0.153

estimate of the stability of the reduced particles in the presence of oxygen at room temperature. Therefore, the samples reduced in the TPR setup were purged with Ar and were cooled to room temperature. After cooling down to room temperature, the reduced sample was oxidized in a (5%O_2 + He) flow (40 cm^3 min^{-1}) in the TPR system for 1 h and was kept in this oxidizing medium overnight. The reoxidized sample was reduced in the TPR run upon heating to 400 °C and keeping at this temperature until hydrogen consumption has ceased. The TPR curves are shown in Fig. 3, and the total hydrogen uptake is given in Table 1. These data indicate that a very slow reoxidation of the supported ruthenium particles occurs at room temperature: only 15% of ruthenium is reoxidized during 24 h. The observed shift of the reduction temperature for the reoxidized catalysts (Figs. 2 and 3) can be explained by the preferential oxidation of the surface of ruthenium particles. The reduction of the second metal on the surface of the presupported (first) metal during the redox synthesis proceeds within a few minutes. Therefore, we can assume on the basis of the TPR experiments that the oxidation of ruthenium by oxygen dissolved in water will be insignificant and the stage of the removal of oxygen from distilled water and solutions for the second metal deposition can be skipped.

The XRD pattern of the gold-ruthenium AuRu5-RR catalyst prepared by the redox method (Fig. 4), except for the lines of the support material, contains also the low-intensity reflections of metallic phases of gold and ruthenium. Since the lines of these phases overlap, it was difficult to calculate the average size of the particles. Oxidation of the AuRu5-RR catalyst by calcination in air at 500 °C for 1 h results in the disappearance of the phase of metallic ruthenium and the appearance of the phase of RuO_2 (Fig. 4), with the average size of the latter being practically the same as in the catalyst prepared by the DPU method. The size of gold particles in this sample is 7 nm, which is considerably lower compared to the sample of the same compositions prepared by the DPU method upon calcinations at 300 °C.

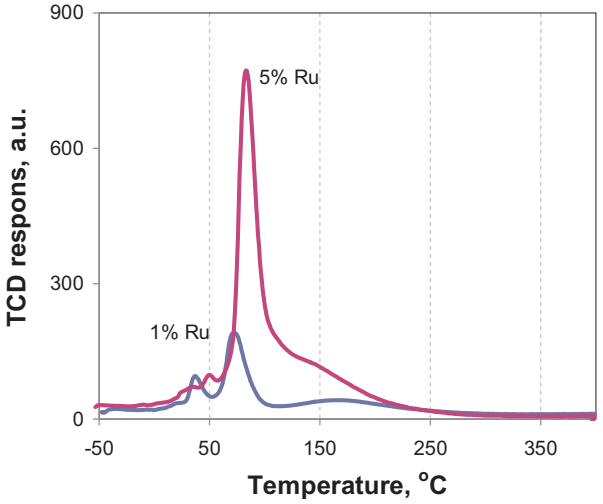

Fig. 3. TPR curves of the samples Ru1 and Ru5 reoxidized at room temperature in the TPR unit after the first TPR run.

Comparison of the value of standard potential for the redox reactions 1–4 [20] is indicative of the possibility of reduction of Au^{3+} by both adsorbed H_2 and Ru^0.

$$[AuCl_4]- + 3e \rightarrow Au^0 + 4Cl^- \quad E^0 = 0.99\,V \tag{1}$$

$$[RuCl_5H_2O]^{2-} + 3e \rightarrow Ru^0 + 5Cl^- + H_2O \quad E^0 = 0.4\,V \tag{2}$$

$$[RuCl_5OH]^{2-} + 4e \rightarrow Ru^0 + 5Cl^- + OH^- \; E^0 = 0.6\,V \tag{3}$$

$$2H^+ - 2e \rightarrow H_2 \; E^0 = 0.0\,V \tag{4}$$

Ruthenium adsorbs hydrogen very actively: the hydrogen-to ruthenium atomic ratio H:Ru previously reported is 0.44–0.75 [23], and the Au^0:Ru molar ratio upon reduction of Au^{3+} by hydrogen adsorbed on Ru should be theoretically close to 0.15–0.25. Therefore, some amount of hydrogen is accumulated at the surface of ruthenium during the cooling process of the reduced sample in a hydrogen flow, i.e. before the introduction of the $H[AuCl_4]$ solution. This amount is higher than the stoichiometric amount with respect to the amount of Au^{3+} ions in the case of the AuRu5-RR catalyst (Au^{3+}:Ru = 0.10) or it is lower in the case of the AuRu1-RR sample (Au^{3+}:Ru = 0.50). As it was established earlier [16], the rate of $[AuCl_4]^-$ reduction to Au^0 by adsorbed hydrogen is two orders of magnitude higher than the rate of the reduction by a noble metal (Pt), therefore the reduction of $[AuCl_4]^-$ to Au^0 in the case of the preparation of the AuRu5-RR catalyst occurs, most likely, by the adsorbed hydrogen without oxidation of Ru. This may result in a uniform deposition of Au on the entire surface of the Ru particle. On the contrary, in the case of the AuRu1-RR sample, the reduction first proceeds with the adsorbed hydrogen, and then by ruthenium, i.e. the deposition of Au occurs predominantly on the atoms with a low coordination number, which, in turn, leads to the formation of larger particles.

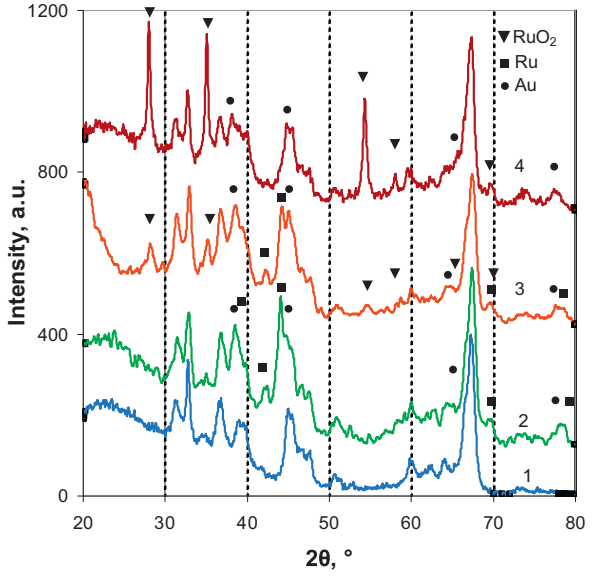

Fig. 4. XRD patterns of the θ-Al_2O_3 (1) and the samples AuRu5-RR initial (2), calcined at 300 °C (3) or at 500 °C (4).

Table 2
The features of the samples.

Sample	Support	Gold deposition procedure	Temperature of calcination (°C)	S_{BET} ($m^2\ g^{-1}$)	Phase composition (the region of coherent scattering)	T_{10} NH3 -T_{90} CO[a], (°C)
Al_2O_3	–	–	1000	95	θ-Al_2O_3 (10 nm)	–
Ru1	θ-Al_2O_3	–	300	90	θ-Al_2O_3 (10 nm); RuO_2 (20 nm)	–
Ru5	θ-Al_2O_3	–	300	88	θ-Al_2O_3 (10 nm); RuO_2 (17 nm)	+30
AuAl	θ-Al_2O_3	DPU	300	95	θ-Al_2O_3 (10 nm)	−60
AuRu1-DPU	Ru1	DPU	300	88	θ-Al_2O_3 (10 nm); RuO_2 (14 nm); Au (>40 nm)	−20
AuRu1-RR	Ru1	RR	None	91	θ-Al_2O_3 (10 nm); Ru^0; Au^0	–
–	–	–	300	–	θ-Al_2O_3 (10 nm); RuO_2; Au^0	+50
AuRu5-DPU	Ru5	DPU	300	89	θ-Al_2O_3 (10 nm); RuO_2 (20 nm); Au (>40 nm)	+30
AuRu5-RR–	Ru5	RR	None	90	θ-Al_2O_3 (10 nm); Ru^0; Au^0	–
–	–	–	300	–	θ-Al_2O_3 (10 nm); Ru^0; RuO_2; Au^0	+100
–	–	–	500	–	θ-Al_2O_3 (10 nm); RuO_2 (18 nm); Au (7 nm)	-

[a] T_{10} NH3 – the temperature of 10% NH_3 conversion; T_{90} CO – the temperature of the 90% CO conversion.

The deposition of gold on the surface of ruthenium in the course of the synthesis of bimetallic Au-Ru catalysts by the redox method is also confirmed by the results of TPR studies of the starting and reoxidized samples. The TPR curve for the AuRu5-RR catalyst reoxidized at 500 °C is shifted towards lower temperatures relative to the TPR curve of RuO_2/θ-Al_2O_3 and exhibits two peaks (Fig. 5), which is accounted for by the influence of gold on the process of reduction of RuO_2 [12]. Since the size of RuO_2 particles is about the same in all the samples (Table 2), the effect of the dispersion of this phase on the reduction process can be excluded. The calculation of the H_2:Ru ratio for this catalyst (Table 1) shows that ruthenium is present in the oxidation state Ru(IV), i.e. the calcination at 500 °C results in the oxidation of the particles of metallic ruthenium to RuO_2, whereas ruthenates and adsorbed oxygen are absent.

The supported gold particles promote the reduction of surface ruthenium oxide at lower temperatures than in the samples Ru5 and AuRu5-DPU reoxidized in the TPR unit (Fig. 6). In this case, the uptake of hydrogen decreases (Table 1), which evidences for the inhibition of ruthenium oxidation by gold, presumably, due to blocking the surface of metallic ruthenium by gold nanoparticles. This is consistent with the fact that the gold particles in the course of the synthesis of Au-Ru catalysts by the redox method are deposited mostly on the surface of metallic ruthenium.

The comparison of the TPR curves of the support material modified by RuO_2 and the sample prepared by depositing gold onto this modified support material using the DPU method shows that the introduction of gold hardly influences the temperature and character of the RuO_2 reduction (Fig. 6). This is also supportive of the predominant deposition of gold as separate particles.

Table 2 summarizes the data obtained by the XRD method and the specific surface areas for all the samples of support materials and catalysts. The specific surface area does not depend on the ruthenium content and the method of gold deposition and coincides with the specific surface area of the starting alumina support. This is an indication of the absence of highly dispersed supported particles.

3.2. Catalytic properties of the catalysts in oxidation of CO and NH3

The catalytic data are presented in Figs. 7 and 8. Oxidation of CO on Au/TiO_2 and Au/θ-Al_2O_3 proceeded in the temperature ranges of 95–185 °C and 155–300 °C, respectively. It should be noted that the Au-Ru catalysts were less active than the Au/TiO_2 catalyst that was used as a benchmark catalyst (Fig. 7), but more active than Au/θ-Al_2O_3. The temperature dependences of the CO conversion on the samples synthesized by the RR and DPU methods can be compared in Fig. 7. The catalysts prepared by the RR method were more active than those obtained by the DPU protocol. A virtually complete conversion of CO was achieved at significantly lower temperatures on the samples prepared by the redox method. Though the RuO_2/θ-Al_2O_3 catalysts also exhibited a rather high activity in CO oxidation, the Au-Ru catalysts, especially those obtained by the redox procedure, were much more active in this reaction. CO oxidation proceeded in the temperature range of 130–195 °C, with the catalysts characterized by a lower Ru loading providing a higher conversion at lower temperatures.

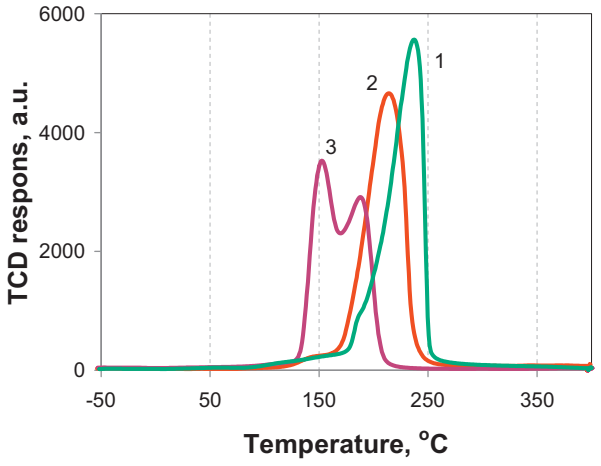

Fig. 5. TPR curves of the initial samples Ru5 (1); AuRu5-DPU (2) and AuRu5-RR calcined at 500 °C (3).

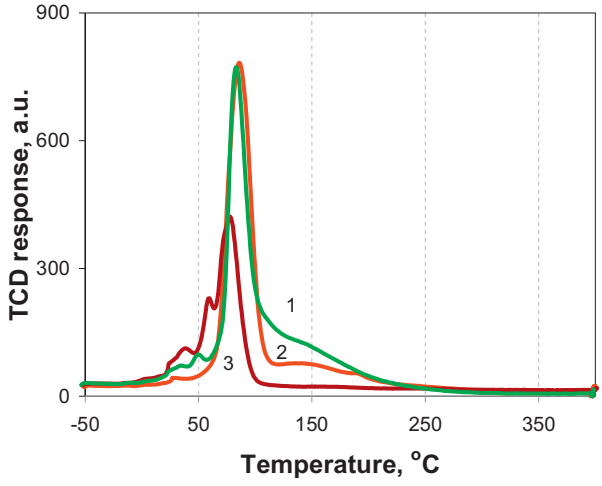

Fig. 6. TPR curves of the samples reoxidized at room temperature in the TPR unit after the first TPR run: Ru5 (1); AuRu5-DPU (2) and AuRu5-RR calcined at 500 °C (3).

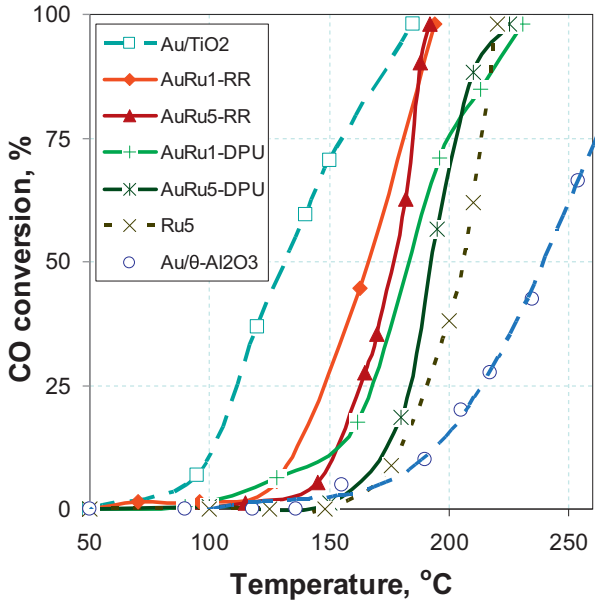

Fig. 7. Temperature dependences of the CO conversion in the gas mixture consisted of 1.5 vol.% NH_3, 4.5 vol.% CO, 22.5 vol.% O_2 and He balance.

For NH_3 oxidation in the CO-containing feed, the prepared Au-Ru catalysts were less active than Au/TiO_2 and $Au/\theta\text{-}Al_2O_3$ (Fig. 8), with the latter catalysts providing an almost complete NH_3 conversion at 360 °C and 400 °C, respectively. These results are opposite to the known facts on NH_3 oxidation in the mixtures without CO. It was reported previously that Ru is a good catalyst of ammonia oxidation below 200 °C [24], whereas Au/TiO_2(P25) catalyzed NH_3 oxidation only at temperatures higher than 350 °C [25].The noticeable conversion in ammonia oxidation on the catalysts prepared by the DPU method was observed already at 150–200 °C, whereas the samples prepared by the RR method catalyzed NH_3 oxidation at the higher temperatures (Fig. 8). The ammonia conversion at 400 °C on the Au-Ru catalysts did not exceed 50%. The temperature dependence of the NH_3 conversion on $RuO_2/\theta\text{-}Al_2O_3$ is close to the curve found for the corresponding Au-containing catalyst. This provides evidence for the predominant NH_3 oxidation on ruthenium sites on the modified support material rather than on the

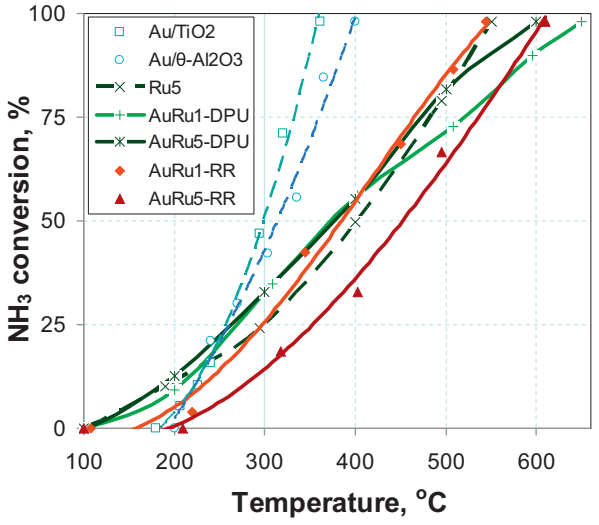

Fig. 8. Temperature dependence of the NH_3 conversion in the gas mixture consisted of 1.5 vol.% NH_3, 4.5 vol.% CO, 22.5 vol.% O_2 and He balance.

gold nanoparticles. The observed ammonia conversion over the θ-Al_2O_3 support in the temperature range 300–400 °C, which value was lower as compared with the conversion over $Au/\theta\text{-}Al_2O_3$ at the same temperatures, indicates that both Au nanoparticles with the size below 3 nm and alumina surface centers contributed in the NH_3 conversion. The lower values of the NH_3 conversion for the AuRu-DPU samples as compared to $Au/\theta\text{-}Al_2O_3$ suggest the blocking effect of the active sites for NH_3 oxidation on the surface of θ-Al_2O_3 by the supported RuO_2, yet the decrease in the catalytic activity in the ammonia oxidation due to the increase in the Au nanoparticle size > 40 nm seems more reasonable. For the least active sample AuRu5-RR, several reasons can explain the decreased activity as compared with $Au/\theta\text{-}Al_2O_3$. The smaller Au particle size of 7 nm, the blocking effect of the relatively large amount of the supported Ru, as well as the lower activity of Au/Ru and Au/RuO_2 systems are among them.

The $1\%Au/5\%Ru/\theta\text{-}Al_2O_3$ catalyst prepared by the RR method revealed the lowest activity in ammonia oxidation.

The high activity of $5\%Au/\gamma\text{-}Al_2O_3$ in ammonia oxidation in the range of 200–400 °C was earlier reported [26] for the ratio $NH_3:O_2 = 1:10$, i.e. close to that used in our study. An equally high activity in NH_3 oxidation was found for the $5\%Au/TiO_2$ and $5\%Au/\gamma\text{-}Al_2O_3$ catalysts at a lower ratio $NH_3:O_2 = 1:1$ [25]. Modification of alumina with alkaline, rare-earth, or transition metal oxides resulted in an enhancement of the activity of Au-containing catalysts in ammonia oxidation [25–27]. As far as we know, the effect of a decreasing activity of the Au/Al_2O_3 catalysts upon preliminary modification of alumina with a transition metal oxide, i.e. ruthenium oxide species, has never been observed previously.

In order to estimate the applicability of the prepared catalysts in the PASS system, the difference between the temperature at which the NH_3 conversion was 10% (T_{10}NH3) and the temperature at which the CO conversion was 90% (T_{90}CO) was calculated for the catalysts. The results of the calculation are presented in Table 2. The high activity in NH_3 oxidation makes impossible the use of the catalyst $1\%Au/\theta\text{-}Al_2O_3$ in the PASS system: the temperature of the 90% CO conversion was 60 °C higher than the temperature of the 10% NH_3 conversion. CO oxidation over this catalyst proceeded simultaneously with ammonia oxidation. The low values of (T_{10}NH3 – T_{90}CO) for the Au–Ru samples prepared by the DPU method indicate a significant NH_3 conversion over the catalyst before the complete CO conversion. Preparation of the Au-Ru/θ-Al_2O_3 catalyst by the redox method resulted in the samples with the large difference (T_{10}NH3 – T_{90}CO). The highest value of 100 °C was obtained for the sample $1\%Au/5\%Ru/\theta\text{-}Al_2O_3$. This catalyst can be recommended for further tests in preferential CO oxidation in the PASS system.

4. Conclusions

Highly active in CO oxidation bimetallic Au-Ru/Al_2O_3 catalysts were prepared by the method of $[AuCl_4]^-$ reduction with hydrogen preadsorbed on a parent monometallic Ru/Al_2O_3 catalyst serving as a carrier. The temperature-programmed reduction studies confirmed a strong interaction between the Au and Ru particles in the samples prepared by this redox method. The redox method was used for the first time in order to prepare the supported Au-Ru catalysts. The redox recipe used in this work allowed us to prepare the alumina-supported gold and ruthenium nanoparticles with an average size below 7 and 18 nm, respectively. When the Au-Ru/θ-Al_2O_3 catalysts were prepared by the conventional deposition-precipitation method with urea, much larger gold particles were formed and, as a result, the contribution of Au particles into CO oxidation decreased dramatically. We found in our study that bimetallic supported Au-Ru/θ-Al_2O_3 catalysts

were more active in CO oxidation than monometallic Au/θ-Al_2O_3 and RuO_2/θ-Al_2O_3 systems. On the contrary, in NH_3 oxidation, the Au-Ru bimetallic samples were less active than the monometallic systems. The enhancement in the catalytic activity in CO oxidation and decrease of the catalytic activity in NH_3 oxidation were the most pronounced for the samples prepared by the redox reaction method.

Acknowledgement

The authors thank Dr. V.D. Nissenbaum for the TG/DTA analyses. The support of the Ministry of Science and Education of the Russian Federation (project no. 11.519.11.5018) is acknowledged.

References

[1] C.H. Kim, K. Perry, M. Viola, W. Li, K. Narayanaswamy, SAE Technical Paper 2011-01-0306 (2011) 452 p.
[2] M.V. Twigg, Catalysis Today 163 (2011) 33–41.
[3] P. Granger, V.I. Parvulescu, Chemical Reviews 111 (2011) 3155–3207.
[4] J. Li, H. Chang, L. Ma, J. Hao, R.T. Yang, Catalysis Today 175 (2011) 147–156.
[5] L. Xu, R.W. McCabe, Catalysis Today 184 (2012) 83–94.
[6] P. Forzatti, I. Nova, E. Tronconi, A. Kustov, J.R. Thøgersen, Catalysis Today 184 (2012) 153–159.
[7] I. Malpartida, O. Marie, P. Bazin, M. Daturi, X. Jeandel, Applied Catalysis B: Environmental 113–114 (2012) 52–60.
[8] G.C. Bond, C. Louis, D. Thompson, Catalysis by Gold, Imperial College Press, London, 2006.
[9] J.-N. Park, J.K. Shon, M. Jin, S.S. Kong, K. Moon, G.O. Park, J.-H. Boo, J.M. Kim, Reaction Kinetics, Mechanisms and Catalysis 103 (2011) 87–99.
[10] S.Y. Chin, O.S. Alexeev, M.D. Amiridis, Applied Catalysis A: General 286 (2005) 157–166.
[11] A. Venugopal, J. Aluha, D. Mogano, M.S. Scurrell, Applied Catalysis A: General 245 (2003) 149–158.
[12] F.-W. Chang, L.S. Roselin, T.-C. Ou, Applied Catalysis A: General 334 (2008) 147–155.
[13] J. Barbier, in: G. Ertl, H. Knözinger, J. Weitkamp (Eds.), Handbook of Heterogeneous Catalysis, Wiley-VCH, Weinheim, 1997, pp. 257–264.
[14] S. Wang, J. He, J. Xie, Y. Zhu, Y. Xie, J.G. Chen, Applied Surface Science 254 (2008) 2102–2109.
[15] I. Bakos, S. Szabó, Journal of Electroanalytical Chemistry 547 (2003) 103–107.
[16] J. Barbier, P. Marécot, G. Del Angel, P. Bosch, J.P. Boitiaux, B. Didillon, J.M. Dominguez, I. Schifter, G. Espinoza, Applied Catalysis A: General 116 (1994) 179–186.
[17] O.A. Kirichenko, V.D. Nissenbaum, G.I. Kapustin, L.M. Kustov, Thermochimica Acta 494 (2009) 35–39.
[18] R. Zanella, S. Giorgio, C.R. Henry, C. Louis, Journal of Physical Chemistry B 106 (2002) 7634–7642.
[19] A. Hugon, N. El Kolli, C. Louis, Journal of Catalysis 274 (2010) 239–250.
[20] S.I. Ginzburg, K.A. Kladyshevskaya, Handbook on Chemical Analysis of Platinum Metals and Gold, Nauka, Moscow, (in Russia), 1965.
[21] A.L. Klyachko-Gurvich, Bulletin of the Russian Academy of Sciences Ser. Khim 10 (1961) 1884–1887.
[22] A. Rochefort, F. Le Peltier, J.P. Boitiaux, Journal of Catalysis 138 (1992) 482–490.
[23] L. Guczi, Catalysis Reviews – Science and Engineering 23 (1981) 329–376.
[24] L.S. Escandón, S. Ordóñez, F.V. Díez, H. Sastre, Reaction Kinetics and Catalysis Letters 76 (2002) 61–68.
[25] S.D. Lin, A.C. Gluhoi, B.E. Nieuwenhuys, Catalysis Today 90 (2004) 3–14.
[26] M.J. Lippits, A.C. Gluhoi, B.E. Nieuwenhuys, Catalysis Today 137 (2008) 446–452.
[27] A.C. Gluhoi, S.D. Lin, B.E. Nieuwenhuys, Catalysis Today 90 (2004) 175–181.